A Closed-Form Rational Model of Coupled Right/Left-Handed Ladder Networks for New Microwave Circuits Design

G. Antonini

Dipartimento di Ingegneria Elettrica e dell'Informazione
Università degli Studi dell'Aquila
Monteluco di Roio, 67040, L'Aquila, Italy
antonini@ing.univaq.it

Abstract – The analytical characterization of coupled composite righ/left-handed ladder networks is presented. Relying on closed-form polynomials, the two-port representation of the composite right/left-handed ladder network is obtained in a rational form, leading to identify its poles and residues and, thus, the state-space macromodel of the network. The proposed macromodel is successfully validated by comparing the numerical results with those obtained using conventional frequency domain techniques of finite periodic structures.

Keywords: Metamaterials, composite righ/left-handed ladder networks, transient analysis, rational macromodeling.

I. INTRODUCTION

Over 30 years ago Veselago [1] theoretically investigated materials with simultaneously negative permittivity and permeability, or left-handed (LH) materials. Recently a transmission line approach of left-handed (LH) materials has been presented in [2, 3] where an equivalent circuit for a left-handed transmission line (LH-TL) is proposed. Such equivalent circuit has been also extended to composite right/left handed (CRLH) metamaterials in [4].

The low insertion loss and broad bandwidth of the LH-TL make it an efficient candidate for microwave frequencies. Due to their negative propagation constant, LH-TLs exhibit phase advance instead of a phase delay as the conventional right-handed transmission lines. This characteristic leads to new designs for many microwave circuits, antennas and couplers.

Artificial CRLH structures are periodic networks whose unit cell consists of a conventional transmission line which is electrically short and loaded with series and shunt elements such that it exhibits a CRLH behavior. Typically the transmission line is loaded by longitudinal (interdigital) capacitances and transverse (short-stub) inductances. As a consequence, the analysis of such type of structures requires modeling either the continuous nature of the transmission line or the discrete behavior of lumped elements. In [5] this task is carried out by solving the Telegrapher's equations for a continuous transmission line problem.

As long as the spatial period of loading lumped elements is electrically short, the resulting structure can be regarded as a finite periodic half-T ladder network (HTLN) which is the best candidate to model composite right/left handed structures.

HTLNs have been widely used in transmission lines modeling [6] under the hypothesis that electrically small sections of length $\Delta\ell$ are assumed ($\Delta\ell \ll \lambda_g$, λ_g being the guided wavelength [3]). In the case of artificial CRLH structures obtained by periodically loading transmission lines or by cascading lumped elements, half-T ladder networks represent their exact model [7, 8].

While a great attention has been devoted to frequency-domain analysis of composite right/left handed structures [3, 9], their time-domain analysis is a relatively new issue. The fact that transient analysis provides information about the system response over many frequencies, makes it attractive to investigate metamaterials properties in a fast and efficient way. In addition, non-linear terminations call for time-domain macromodels.

Time-domain transmission line matrix (TLM) modeling of metamaterials with negative refractive index has been derived in [10]. A composite right/left-handed equivalent circuit FDTD method is presented in [11] and applied to investigate several transient and refractive phenomena occurring at the interface between a CRLH metamaterial and a purely right-handed (PRH) structure. More recently, a stability analysis of 1-D double negative transmission lines is presented in [5] where a method of moments (MOM) [12] approach is employed to perform time-domain computations.

In [13] a systematic approach to composite righ/left-handed ladder networks (CRLH-LNs) has been presented. The aim of this work is to extend such a methodology to coupled composite righ/left-handed ladder networks. Metamaterial coupled-line couplers have the advantage of providing arbitrary coupling level in addition to the broad bandwidth of conventional coupled-line couplers. A comprehensive frequency-domain analysis of this type of structures is presented in [14] where mechanisms of

coupling are derived in the framework of generalized transmission lines.

Based on the ladder structure of the system, a rigorous analysis of coupled CRLH-LNs is developed, which is based on closed-form polynomials, leading to a rational macromodel of the transfer functions of the system. In the recent years new and effective techniques have been developed to generate macromodels from frequency-domain response of electromagnetic systems [15–17]. CRLH-LN structures can be regarded as periodic and finite; as a consequence, any electrical quantities of the CRLH-LNs, such as voltages and currents, can always be expressed in a rational form due to the RLCG nature of the network. This target is achieved by using closed-form polynomials depending on the cell matrix $\boldsymbol{K}(s) = \boldsymbol{Y}_2(s)\boldsymbol{Z}_1(s)$ of the ladder network. Polynomial coefficients are *a-priori* analytically computed and stored. The resulting rational macromodel is the exact representation of the CRLH-LN and can be used for both time and frequency-domain analysis of coupled CRLH-LNs.

The paper is organized as follows: Section II presents the polynomial model of CRLH ladder networks leading to a rational multiport representations of coupled CRLH-LNs, described in Section III, which is suitable for an efficient computation of poles/residues and, thus, for a time-domain macromodel. Section IV presents the computation of the dispersion diagram and a comparison with that of CRLH-TLs. Numerical tests are carried out and reported in Section V. The conclusions are drawn in Section VI.

II. POLYNOMIAL MODEL OF CRLH-LNS

Composite right/left handed transmission lines can be modeled as the cascade of n elementary identical half-T cells, as shown in Fig. 1, characterized by both longitudinal and transversal inductances and capacitances [4]. In addition, longitudinal resistances and transverse conductances are added to take the ever existing losses into account.
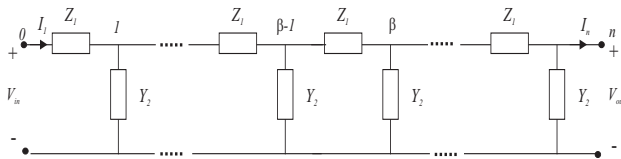

Fig. 1.   Half-T ladder network.

The resulting structure is a *high-pass* filter mimicking a composite right/left handed transmission line. The equivalent circuit shown in Fig. 2 represents a possible model of a cell although other topologies can be considered [2].

The transmission line model can still be adopted under the hypothesis that the unit cell is electrically small [2, 18], but a rigorous analysis of practical realizations of

CRLH structures is desirable and useful to designers. The main difference with respect to the continuous transmission line model relies on the fact that the half-T ladder network is a periodic structure which is characterized by having any transfer function to be written as rational function. Obviously, standard multiport network theory can be used to analyze the ladder network in the frequency domain [19] but such an approach is not suitable to provide a time-domain macromodel.
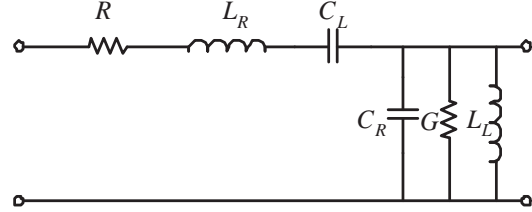

Fig. 2.   Elementary half-T cell for a composite right/left handed ladder network (CRLH-LN).

To the aim to develop the closed-form macromodel of a CRLH-LN, is useful to define the unit cell impedance and admittance in the Laplace domain,

$$Z_1(s) = R + sL_R + \frac{1}{sC_L} = \frac{s^2 L_R C_L + sRC_L + 1}{sC_L}$$

$$Y_2(s) = G + sC_R + \frac{1}{sL_L} = \frac{s^2 L_L C_R + sGL_L + 1}{sL_L},$$
(1a)

which are rational functions.

In [20] it is shown that, in the hypothesis of a uniform, linear and time invariant HTLN, the voltage at the generic node β in the Laplace-domain can be expressed as,

$$V_\beta(s) = \frac{P_b^{n-\beta}(K(s))}{P_b^n(K(s))} V_{in}(s)$$
(2)

where the cell factor $K(s)$ is,

$$K(s) = Y_2(s) Z_1(s)$$
(3)

and

$$P_b^{n-\beta}(K(s)) = \sum_{j=0}^{n-\beta} b_{j,n-\beta} K^j(s)$$
(4)

is a polynomial in $K(s)$, of order $n-\beta$ with $0 \le \beta \le n$. Polynomial coefficients b are generated as [21],

$$b_{i,j} = \begin{pmatrix} i+j \\ j-i \end{pmatrix} = \begin{pmatrix} i+j \\ 2j \end{pmatrix}$$
(5)

which leads to the generation of the following triangle known as DFF triangle [20], shown in Table II.

The general expression of the longitudinal branch current $I_{\beta 1}(s)$ is,

$$I_{\beta 1}(s) = \frac{1}{Z_1(s)} \frac{P_c^{n-\beta+1}(K(s))}{P_b^n(K(s))} V_{in}(s)$$
(6)

Table 1. DFF triangle.

i^j	0	1	2	3	4
0	1				
1	1	1			
2	1	3	1		
3	1	6	5	1	
4	1	10	15	7	1
...	....				

where the corresponding roots are,

$$P_c^{n-\beta+1}\left(K(s)\right) = \sum_{j=0}^{n-\beta+1} c_{j,n-\beta+1}K^{j+1}(s) \quad (7)$$

is a polynomial in $K(s)$ of order $n - \beta + 1$ and the coefficients c are obtained as [21],

$$c_{i,j} = \begin{pmatrix} i+j+1 \\ j-i \end{pmatrix} = \begin{pmatrix} i+j+1 \\ 2j+1 \end{pmatrix} \quad (8)$$

leading to the triangle known as DFFz triangle [20], shown in Table II.

Table 2. DFFz triangle.

i^j	0	1	2	3	4
0	1				
1	1	1			
2	1	3	1		
3	1	6	5	1	
4	1	10	15	7	1
...	....				

It is worth noticing that polynomials $P_b^n(K(s))$ and $P_c^n(K(s))$ allow to describe any kind of finite periodic structure, provided the cell factor $K(s)$ is given. In particular it can be used to model CRLN-LNs.

III. COUPLED CRLN-LNS

As stated before, no assumption is done either on the cell factor $K(s)$ as for the nature of longitudinal impedance $\boldsymbol{Z}_1(s)$ and transverse admittance $\boldsymbol{Y}_2(s)$ or its dimension; hence, the extension to the multidimensional case is straightforward. To this aim, let us consider N coupled CRLH-LNs (Fig. 3 shows an example with $N = 2$) and define the longitudinal impedance and transverse admittance matrices as,

$$\boldsymbol{Z}_1(s) = \boldsymbol{R} + s\boldsymbol{L}_R + \frac{1}{s}\boldsymbol{C}_L^{-1} \quad (9a)$$

$$\boldsymbol{Y}_2(s) = \boldsymbol{G} + s\boldsymbol{C}_R + \frac{1}{s}\boldsymbol{L}_L^{-1}, \quad (9b)$$

where $\boldsymbol{R}$ and $\boldsymbol{G}$ are diagonal matrices containing the resistance and conductance of each half-T cell, $\boldsymbol{L}_R$ and $\boldsymbol{C}_R$ are the right-handed inductance and capacitance matrices and $\boldsymbol{L}_L$ and $\boldsymbol{C}_L$ are the left-handed inductance
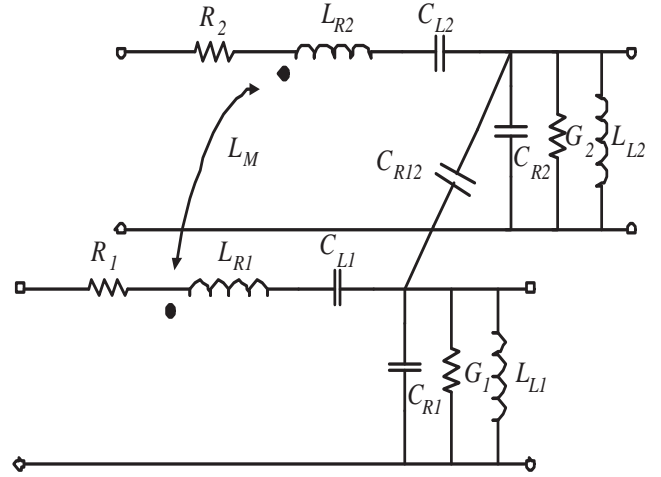

Fig. 3. Elementary half-T cell for a coupled composite right/left handed ladder network (CRLH-LN).

and capacitance matrices, respectively. These latter are diagonal matrices.

In the multidimensional case, the cell factor $\boldsymbol{K}(s)$ becomes a matrix and can be defined as,

$$\boldsymbol{K}(s) = \boldsymbol{Y}_2(s)\boldsymbol{Z}_1(s). \quad (10)$$

The polynomials $P_b^n(K(s))$ and $P_c^n(K(s))$ become polynomial matrices,

$$P_b^n(\boldsymbol{K}(s)) = \sum_{j=0}^{n} b_{j,n}\boldsymbol{K}^j(s) \quad (11a)$$

$$P_c^n(\boldsymbol{K}(s)) = \sum_{j=0}^{n} c_{j,n}\boldsymbol{K}^{j+1}(s). \quad (11b)$$

When general terminal conditions need to be considered, the chain parameters [6] of the half-T ladder network can be obtained as,

$$\boldsymbol{\Phi}_{11}(s) = \sum_{j=0}^{n-1} b_{j,n-1}\boldsymbol{K}^j(s) = P_b^{n-1}(\boldsymbol{K}(s)), (12a)$$

$$\boldsymbol{\Phi}_{12}(s) = -\left(\sum_{j=0}^{n} c_{j,n}\boldsymbol{K}^{j+1}(s)\right)\cdot\boldsymbol{Y}_2^{-1}(s) \quad (12b)$$
$$= -P_c^n(\boldsymbol{K}(s))\cdot\boldsymbol{Y}_2^{-1}(s),$$

$$\boldsymbol{\Phi}_{21}(s) = -\left(\sum_{j=0}^{n} c_{j,n}\boldsymbol{K}^{j+1}(s)\right)\cdot\boldsymbol{Z}_1^{-1}(s) \quad (12c)$$
$$= -P_c^n(\boldsymbol{K}(s))\cdot\boldsymbol{Z}_1^{-1}(s),$$

$$\boldsymbol{\Phi}_{22}(s) = \sum_{j=0}^{n} b_{j,n}\boldsymbol{K}^j(s) = P_b^n(\boldsymbol{K}(s)). \quad (12d)$$

Polynomials $P_b^{n-1}(\boldsymbol{K}(s))$ and $P_c^n(\boldsymbol{K}(s))$ can be factored into zero-pole pairs. Their factorization is accomplished by using the poles given by the expressions

presented in [21],

$$P_b^{n-1}(\boldsymbol{K}(s)) = \prod_{j=1}^{n-1} (\boldsymbol{K}(s) - u_{j,n-1}\boldsymbol{U}_N) \quad (13a)$$

$$P_c^{n}(\boldsymbol{K}(s)) = \prod_{j=1}^{n-1} (\boldsymbol{K}(s) - v_{j,n-1}\boldsymbol{U}_N) \cdot \boldsymbol{K}(s), \quad (13b)$$

where $\boldsymbol{U}_N$ is the identity matrix of order N and polynomial roots $u_{j,n}$ and $v_{j,n}$ can be computed analytically as,

$$u_{j,n} = -4\sin^2\left[\frac{(2j-1)}{(2n+1)}\frac{\pi}{2}\right] \quad (14a)$$

$$v_{j,n} = -4\sin^2\left[\frac{j}{(n+1)}\frac{\pi}{2}\right], \quad (14b)$$

for $j = 1\cdots n$.

The knowledge of the chain parameters Φ allows to obtain the rational form of any other two port matrix representation. The $\boldsymbol{Z}(s)$ matrix entries can be evaluated in terms of $P_b^n(\boldsymbol{K}(s))$ and $P_c^n(\boldsymbol{K}(s))$ polynomials as,

$$\boldsymbol{Z}_{11}(s) = P_b^n(\boldsymbol{K}(s)) \cdot \left(P_c^n(\boldsymbol{K}(s)) \cdot \boldsymbol{Z}_1^{-1}(s)\right)^{-1}(15a)$$

$$\boldsymbol{Z}_{12}(s) = -\left(P_c^n(\boldsymbol{K}(s)) \cdot \boldsymbol{Z}_1^{-1}(s)\right)^{-1}, \quad (15b)$$

$$\boldsymbol{Z}_{21}(s) = -\left(P_c^n(\boldsymbol{K}(s)) \cdot \boldsymbol{Z}_1^{-1}(s)\right)^{-1}, \quad (15c)$$

$$\boldsymbol{Z}_{22}(s) = P_b^{n-1}(\boldsymbol{K}(s)) \cdot \left(P_c^n(\boldsymbol{K}(s))\boldsymbol{Z}_1(s)^{-1}\cdot\right)^{-1}. \quad (15d)$$

The previous expressions (15a)- (15d), taking into account that $\boldsymbol{K}(s) \cdot \boldsymbol{Y}_2^{-1}(s) = \boldsymbol{Z}_1(s)$, can be factored in the following way,

$$\boldsymbol{Z}_{11}(s) = \prod_{j=1}^{n} (\boldsymbol{K}(s) - u_{j,n-1}\boldsymbol{U}_N)$$
$$\cdot \left[\prod_{j=1}^{n-1} (\boldsymbol{K}(s) - v_{j,n-1}\boldsymbol{U}_N) \cdot \boldsymbol{Y}_2(s)\right]^{-1}(16a)$$

$$\boldsymbol{Z}_{21}(s) = \boldsymbol{Z}_{12}$$
$$= -\left[\prod_{j=1}^{n-1} (\boldsymbol{K}(s) - v_{j,n-1}) \cdot \boldsymbol{Y}_2(s)\right]^{-1} \quad (16b)$$

$$\boldsymbol{Z}_{22}(s) = \prod_{j=1}^{n-1} (\boldsymbol{K}(s) - u_{j,n-1}\boldsymbol{U}_N)$$
$$\cdot \left[\prod_{j=1}^{n-1} (\boldsymbol{K}(s) - v_{j,n-1}\boldsymbol{U}_N) \cdot \boldsymbol{Y}_2(s)\right]^{-1}(16c)$$

The poles of the open-ended CRLH-LN are obtained as the zeros of the following equation,

$$\mathcal{P}(s) = \det\left[\prod_{j=1}^{n-1} (\boldsymbol{K}(s) - v_{j,n-1}\boldsymbol{U}_N) \cdot \boldsymbol{Y}_2(s)\right] = 0$$
$$(17)$$

which can be rewritten as,

$$\prod_{j=1}^{n-1} \det\left[\boldsymbol{K}(s) - v_{j,n-1}\boldsymbol{U}_N\right] \cdot \det\left[\boldsymbol{Y}_2(s)\right] = 0. \quad (18)$$

The poles of the CRLH-LN can be identified as,

1) the roots of polynomial,

$$\det\left[\boldsymbol{Y}_2(s)\right]. \quad (19)$$

2) the roots of polynomials,

$$\det\left[\boldsymbol{Y}_2(s)\boldsymbol{Z}_1(s) - v_{j,n-1}\boldsymbol{U}_N\right], \quad j = 1\cdots n-1. \quad (20)$$

Residues of the i-th pole can be obtained as,

$$\boldsymbol{R}_{11,i} = \quad (21)$$
$$\prod_{j=1}^{n} (\boldsymbol{K}(s) - u_{j,n-1}\boldsymbol{U}_N) \cdot (s - p_i)|_{s=p_i}$$
$$\cdot \text{adj}\left[\prod_{j=1}^{n-1} (\boldsymbol{K}(s) - v_{j,n-1}\boldsymbol{U}_N)\boldsymbol{Y}_2(s)\right]/\mathcal{P}(s)$$

$$\boldsymbol{R}_{12,i} =$$
$$-\text{adj}\left[\left(\prod_{j=1}^{n-1} (\boldsymbol{K}(s) - v_{j,n-1}\boldsymbol{U})\right)\boldsymbol{Y}_2(s)\right]/\mathcal{P}(s)$$
$$\cdot (s - p_i)|_{s=p_i}, \quad (22)$$

$$\boldsymbol{R}_{21,i} =$$
$$\text{adj}\left[\left(\prod_{j=1}^{n-1} (\boldsymbol{K}(s) - v_{j,n-1}\boldsymbol{U})\right)\boldsymbol{Y}_2(s)\right]/\mathcal{P}(s)$$
$$\cdot (s - p_i)|_{s=p_i}, \quad (23)$$

$$\boldsymbol{R}_{22,i} =$$
$$\prod_{j=1}^{n-1} (\boldsymbol{K}(s) - u_{j,n-1}\boldsymbol{U}_N) \cdot (s - p_i)|_{s=p_i}$$
$$\cdot \text{adj}\left[\prod_{j=1}^{n-1} (\boldsymbol{K}(s) - v_{j,n-1}\boldsymbol{U}_N)\boldsymbol{Y}_2(s)\right]/\mathcal{P}(s),(24)$$

for $i = 1\cdots P_Z$, being P_Z the total number of poles of the $\boldsymbol{Z}$ matrix entries and adj indicates the adjugate operator. The reciprocity of the LN guarantees that matrices $\boldsymbol{R}_{21,i} = \boldsymbol{R}_{12,i}$.

A. Remarks

If we consider two identical coupled HTLNs some observations can be addressed when computing poles of equation (20). In fact, in this case, the diagonal elements of all matrices are identical and exists a unique nonsingular transformation which diagonalizes both matrices $\boldsymbol{L}_R$ and $\boldsymbol{C}_R$. As stated before, matrices $\boldsymbol{R}, \boldsymbol{G}, \boldsymbol{C}_L$ and $\boldsymbol{L}_L$ are already diagonal. The transformation is,

$$\boldsymbol{T} = \frac{1}{\sqrt{2}}\begin{bmatrix} 1 & 1 \\ 1 & -1 \end{bmatrix}. \quad (25)$$

Hence, multiplying the original matrix $\boldsymbol{Y}_2\left(s\right)\boldsymbol{Z}_1\left(s\right)$ in equation (20) on the left by $\boldsymbol{T}^{-1}$ and on the right by $\boldsymbol{T}$, the determinant remains the same since $\boldsymbol{T}$ is nonsingular and can be written as,

$$\det\left[\boldsymbol{T}^{-1}\boldsymbol{Y}_2\left(s\right)\boldsymbol{Z}_1\left(s\right)\boldsymbol{T} - v_{j,n-1}\boldsymbol{U}_2\right] = \quad (26)$$

$$\det\left[\left(\boldsymbol{R} + \boldsymbol{T}^{-1}\boldsymbol{L}_R\boldsymbol{T} + \frac{1}{s}\boldsymbol{C}_L^{-1}\right)\right. \quad (27)$$

$$\left.\cdot\left(\boldsymbol{G} + \boldsymbol{T}^{-1}\boldsymbol{C}_R\boldsymbol{T} + \frac{1}{s}\boldsymbol{L}_L^{-1}\right) - v_{j,n-1}\boldsymbol{U}_2\right].$$

From equation (26), it is worth noticing that poles of equation (20) can be computed as the roots of two quartic equations,

$$\det\left[\tilde{Z}_{1c}\tilde{Y}_{2c} - v_{j,n-1}\right] = 0 \quad (28a)$$

$$\det\left[\tilde{Z}_{1d}\tilde{Y}_{2d} - v_{j,n-1}\right] = 0, \quad (28b)$$

where

$$\tilde{Z}_{1c} = R + s\left(L_R + L_M\right) + \frac{1}{s}C_L^{-1}, \quad (29a)$$

$$\tilde{Y}_{2c} = G + s\left(C_R + C_M\right) + \frac{1}{s}L_L^{-1}, \quad (29b)$$

$$\tilde{Z}_{1d} = R + s\left(L_R - L_M\right) + \frac{1}{s}C_L^{-1}, \quad (29c)$$

$$\tilde{Y}_{2d} = G + s\left(C_R - C_M\right) + \frac{1}{s}L_L^{-1}, \quad (29d)$$

and L_R, L_M represents the self and mutual inductance of the lines, C_R, C_M represents the self and mutual capacitance of the lines, respectively.

Hence, the poles of the coupled CRLH-LN can be computed by solving two quartic algebraic equations corresponding to two separate CRLH-LNs, characterized by common and differential mode right-handed parameters. The quartic equations (28) can be analytically solved using the method described in [22]. Since the system is physically stable, the exact solution of equations (28) ensures the stability of both the decoupled and coupled CRLH-LNs because the transformation (25) is purely real.

It is also to be pointed out that the proposed method is general as far as the topology and nature of impedance $\boldsymbol{Z}_1$ and admittance $\boldsymbol{Y}_2$ which can be eventually dispersive.

In [8] an equivalent circuit is used to model double-negative metamaterial lenses; recursive relations are provided giving the node voltages and branch currents and the link with the Fibonacci problem is pointed out. The proposed method completely exploits the polynomial nature of the problem, leading to closed-form models of CRLH-LNs. The polynomial coefficients reduce to Fibonacci's numbers when $\boldsymbol{Z}_1(s) = \boldsymbol{Y}_2(s)^{-1}$ so that $\boldsymbol{K}(s) = \boldsymbol{I}_N$ [20].

B. Rational macromodel

The explicit knowledge of poles and residues allow to select the dominant poles according to the frequency range of interest; among the selected poles, only those whose residues significantly impact the frequency response are retained. This two-step process leads to generate a reduced order model of the CRLH-LN.

The poles-residues representation of the impedance matrix $\boldsymbol{Z}$ allows to generate a macromodel in the state-space form, leading to a set of first order differential equations which reads,

$$\frac{d}{dt}\mathbf{x}\left(t\right) = \mathcal{A}\mathbf{x}\left(t\right) + \mathcal{B}\mathbf{u}\left(t\right)$$

$$\mathbf{y}\left(t\right) = \mathcal{C}\mathbf{x}\left(t\right) + \mathcal{D}\mathbf{u}\left(t\right), \quad (30)$$

where $\mathcal{A} \in \mathrm{R}^{p\times p}$, $\mathcal{B} \in \mathrm{R}^{p\times q}$, $\mathcal{C} \in \mathrm{R}^{q\times p}$, $\mathcal{D} \in \mathrm{R}^{q\times q}$, p is the number of states and q is the number of ports. Since the impedance matrix representation is used, the input and the output vectors, $\mathbf{u}\left(t\right)$ and $\mathbf{y}\left(t\right)$ respectively, correspond to port currents $\boldsymbol{i}\left(t\right)$ and voltages $\boldsymbol{v}\left(t\right)$, respectively. The set of first order differential equations (30) are completed with the terminal conditions and solved numerically.

It is to be remarked that the proposed macromodeling methodology can be used for longitudinal impedance $\boldsymbol{Z}_1(s)$ and transverse admittance $\boldsymbol{Y}_2(s)$ different from the series ones of equations (9a) and (9b) (e.g. see [2]).

IV. DISPERSION RELATION OF THE PERIODIC CRLH-LN

The dispersion relation of a CRLH-LN is obtained by applying periodic boundary conditions to the unit cell represented by its $ABCD$ matrix. As a consequence, the output voltages and currents are related to the input voltages and currents by the propagation term $e^{-\gamma\ell}$, being ℓ the length of each cell. Hence, in the multidimensional case, according to the Bloch-Floquet theorem, the following relations hold,

$$\begin{bmatrix} \boldsymbol{A} & \boldsymbol{B} \\ \boldsymbol{C} & \boldsymbol{D} \end{bmatrix} \cdot \begin{bmatrix} \boldsymbol{V}_{in} \\ \boldsymbol{I}_{in} \end{bmatrix} = \psi \begin{bmatrix} \boldsymbol{V}_{in} \\ \boldsymbol{I}_{in} \end{bmatrix} \quad (31)$$

which is an eigensystem with eigenvalues $\psi_n = e^{-\gamma_n\ell}$. For a half-T unit cell, $ABCD$ parameters are,

$$\boldsymbol{A} = \boldsymbol{I}_N + \boldsymbol{Z}_1\boldsymbol{Y}_2 \quad (32a)$$

$$\boldsymbol{B} = \boldsymbol{Z}_1, \quad (32b)$$

$$\boldsymbol{C} = \boldsymbol{Y}_2, \quad (32c)$$

$$\boldsymbol{D} = \boldsymbol{I}_N. \quad (32d)$$

The computation of the eigenvalues ψ_n leads to determine the dispersion relations. The eigensystem (31) can be rewritten as a homogeneous linear system which must have a zero determinant to provide non trivial solution [3]. For coupled CRLH-LNs, the eigenvalues ψ_n are computed as the solution of the following equation,

$$\det\begin{bmatrix} \boldsymbol{A} - \psi_n & \boldsymbol{B} \\ \boldsymbol{C} & \boldsymbol{D} - \psi_n \end{bmatrix} = 0. \quad (33)$$

From its solutions ψ_n, the propagation constants are obtained as,

$$\gamma_n = -\frac{1}{\ell}\log\psi_n \tag{34a}$$

$$\alpha_n = \text{Re}(\gamma_n), \tag{34b}$$

$$\beta_n = \text{Im}(\gamma_n). \tag{34c}$$

For a single CRLH-LN with a half-T unit cell, it is trivial finding,

$$\gamma = -\frac{1}{\ell}\log\left(1 + \frac{Z_1 Y_2}{2} \pm \sqrt{\left(1 + \frac{Z_1 Y_2}{2}\right)^2 - 1}\right) \tag{35}$$

where ℓ is the length of each section.

In [4] it is shown that CRLH-LN is equivalent to the homogenous CRLH-TL for small electrical lengths and the dispersion relation obtained applying periodic boundary conditions reduces to the homogenous dispersion relation. Since such a condition holds only within a limited frequency range, the transmission line model cannot be used for accurate broadband time-domain analysis of CRLH-LN structures. In fact, due to the left-handed lumped elements C_L and L_L, for a fixed length ℓ, the imaginary part of the propagation constant greatly differs, at low frequencies, from that of the transmission line, as confirmed by the numerical results in the next section.

V. NUMERICAL RESULTS

A. Dispersion diagram analysis

To the aim of investigating the difference between the continuous and the periodic structures, the CRLH-LN described in [4] has been considered. It is characterized by global parameters $R = 10^{-3}\ \Omega$, $L_R = 2.45$ nH, $C_L = 0.68$ pF, $G = 10^{-3}$ S, $C_R = 0.5$ pF and $L_L = 3.38$ nH; 10 unit cells have been considered of length $\ell = 6.1$ mm.

Figure 4 shows the dispersion diagram of the CRLH-LN described in ([4], page 41) using the Bloch-Floquet theorem [3], the approximated one under the hypothesis of electrically small sections and that of a homogeneous CRLH-TL. It is seen that the hypothesis of electrically small network leads to significantly different results from the Bloch-Floquet theorem in the gigahertz range.

This result is expected since the wavelength is inversely proportional to the phase constant β. At frequencies below 1 GHz the phase constant of the CRLN-LN is larger than that of the CRLH-TL, leading to smaller wavelengths. Figure 5 shows the phase velocity diagram. Again, a significant difference is observed, below 1 GHz, between the result of the Bloch-Floquet theorem and those obtained assuming the hypothesis of electrically small sections.

Figure 6 shows the attenuation constant as evaluated using the homogeneous CRLH-TL and the discrete
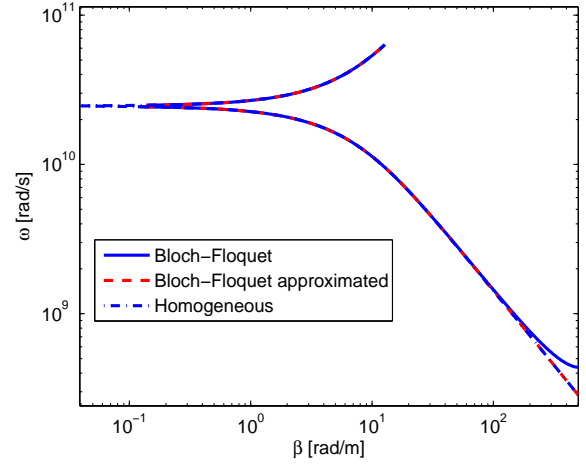

Fig. 4. Dispersion diagram. The solid line refers to the Bloch-Floquet theorem, the dashed line refers to the approximation under the hypothesis of electrically small network, the dashdot line refers to the homogeneous CRLN-TL (example V-A).
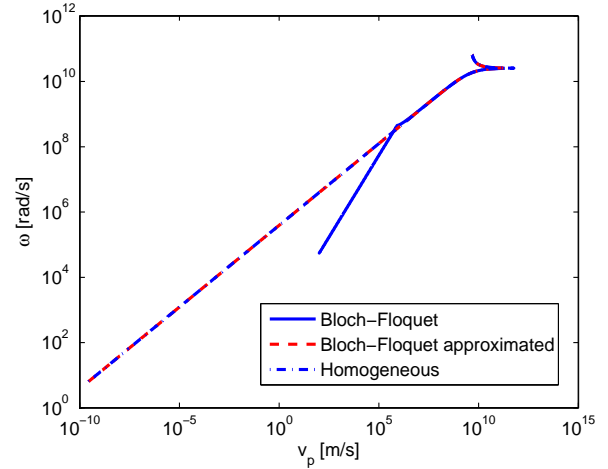

Fig. 5. Phase velocity diagram. The solid line refers to the Bloch-Floquet theorem, the dashed line refers to the approximation under the hypothesis of electrically small sections, the dashdot line refers to the homogeneous CRLN-TL (example V-A).

CRLH-LN models. A significant difference is observed up to few gigahertz.

The previous results point out that the homogeneous CRLH-TL may be not accurate at low frequencies and may generate inaccuracies when adopted for broadband macromodeling of CRLH-LN structures.

Figure 7 shows the poles in the complex plane. A large number of poles is clustered close to zero and determine the left handed low frequency oscillatory behavior of the response. The selection of dominant poles may be a

difficult task due to the presence of many clustered poles which leads to ill-conditioning.
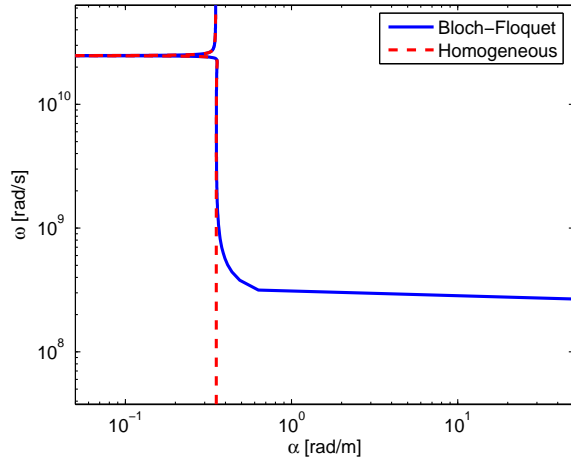

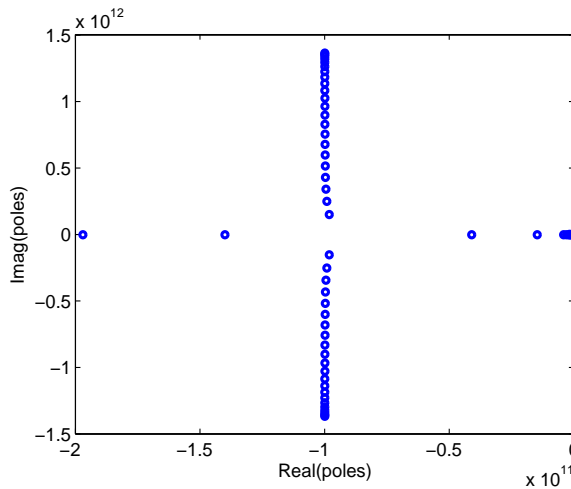Fig. 6. Attenuation constant (example V-A).

Fig. 7. Location of poles in the complex plane (example V-A).

The chain parameters of the CRLH-LN of order 10 have been computed using the proposed polynomial method and compared with those obtained by inversion of the global transmission matrix computed as cascade of ten identical sections and those of the equivalent CRLH-TL. Figure 8 shows the magnitude spectrum of Φ_{11} up to 0.5 GHz. It is clearly seen that the polynomial approach is in a very good agreement with the result of the CRLH-LN while, again, the equivalent CRLH-TL exhibits a significant difference.

The CRLH-LN has been excited by a pulse with 100 ps rise and fall times and width 5 ns. The input is terminated on 50 Ω resistance, the output port is left open. Figure 9 shows a sample of the output voltage as evaluated

using the equivalent CRLH-TL model via IFFT, the half-T ladder network via IFFT and the proposed time-domain macromodel.
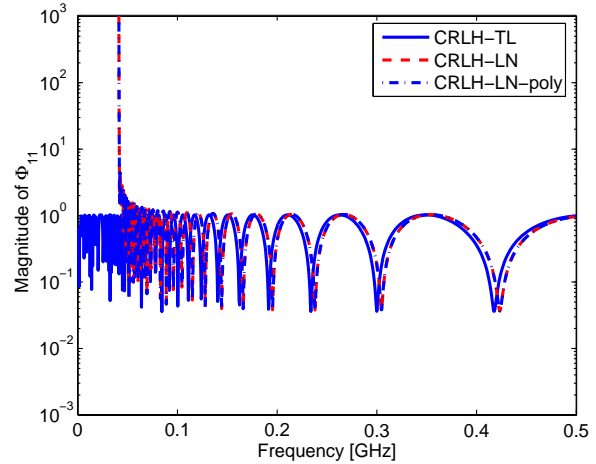
Fig. 8. Chain parameter Φ_{11}. The solid line refers to the equivalent CRLH-TL, the dashed line refers to the result obtained by inversion of the global transmission matrix, the dashdot line refers to the proposed polynomial approach (example V-A).
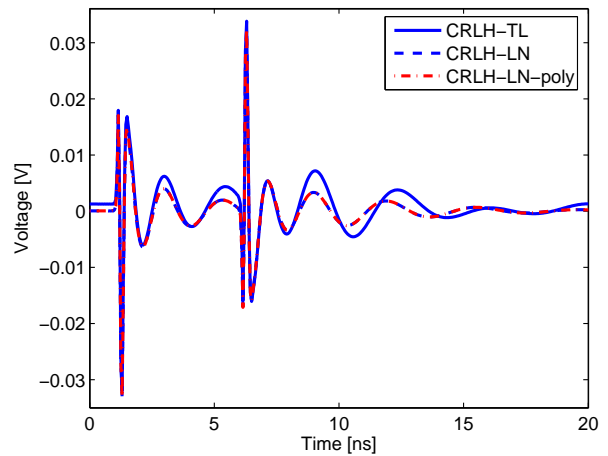

Fig. 9. Output voltage. The solid line refers to the equivalent CRLH-TL via IFFT, the dashed line refers to the result obtained by inversion of the CRLH-LN model via IFFT, the dashdot line refers to the proposed time-domain macromodel (example V-A).

As before, the polynomial-based macromodeling approach is in perfect agreement with the analysis of the global ladder network while the equivalent CRLH-TL exhibits a significant difference. In particular, the CRLH-LN is characterized by a larger attenuation than the CRLH-TL, as expected from Fig. 6. Furthermore, the use

of the IFFT, combined with a underestimated attenuation, causes a not accurate *dc* value of the CRLH-TL results.

B. Two coupled CRLH-LNs

In the second example a coupled CRLH-LN is considered. It is constituted by 40 half-T cells with parameters $L_{R1} = L_{R2} = 1.938$ nH, $C_{R1} = C_{R2} = 0.841$ pF, $L_{L1} = L_{L2} = 0.749$ nH, $C_{L1} = C_{L2} = 0.416$ pF, $L_M = 0.361$ nH, $C_M = -0.189$ pF, $R_1 = R_2 = 10$ mΩ, $G_1 = G_2 = 1$ mΩ. The coupled ladder networks are terminated on 50 Ω resistances at the input ports and 1.5 pF capacitances at the output ports. The rational macromodel has been generated leading to 316 poles; among them only 172 have been selected as dominant in the 0-20 GHz range. Figure 10 shows the location of poles in the complex plane: the circles refer to the set of poles of the CRLH-LN, the stars to those selected as dominant.

Fig. 11.   Magnitude of residues of impedance Z_{13} (example V-B).

Fig. 10.   Location of poles in the complex plane (example V-B).

Figure 11 reports the magnitude of the corresponding residues: circles refer to the set of poles computed by equations (19) and (20), stars indicate those selected as dominant in the frequency range of interest.

A sample of the magnitude and phase spectra of the impedances Z_{11} and Z_{12} is presented in Figs. 12 and 13. For the sake of comparison impedances are computed using both the polynomial (HTLN-pol) and the pole/residue (HTLN-RP) forms; as seen, a perfect agreement is obtained.

The knowledge of poles and residues of the HTLN has allowed to generate a rational macromodel in a state-space form. Figure 14 shows the transient voltage at the input port of the second line as evaluated by using the standard frequency-domain model combined with the IFFT to obtain the time-domain results and the proposed reduced macromodel; as seen, no significant difference is observed.
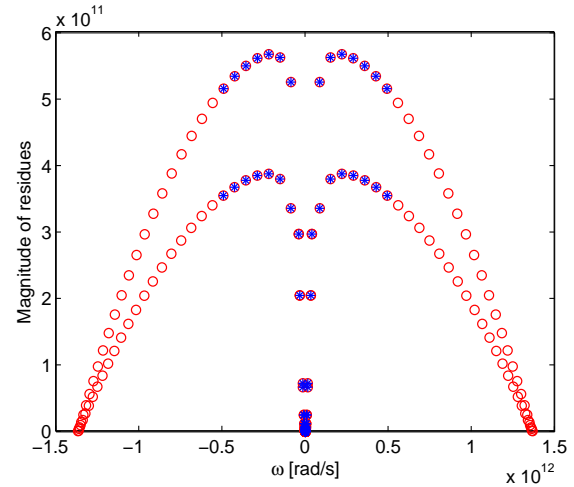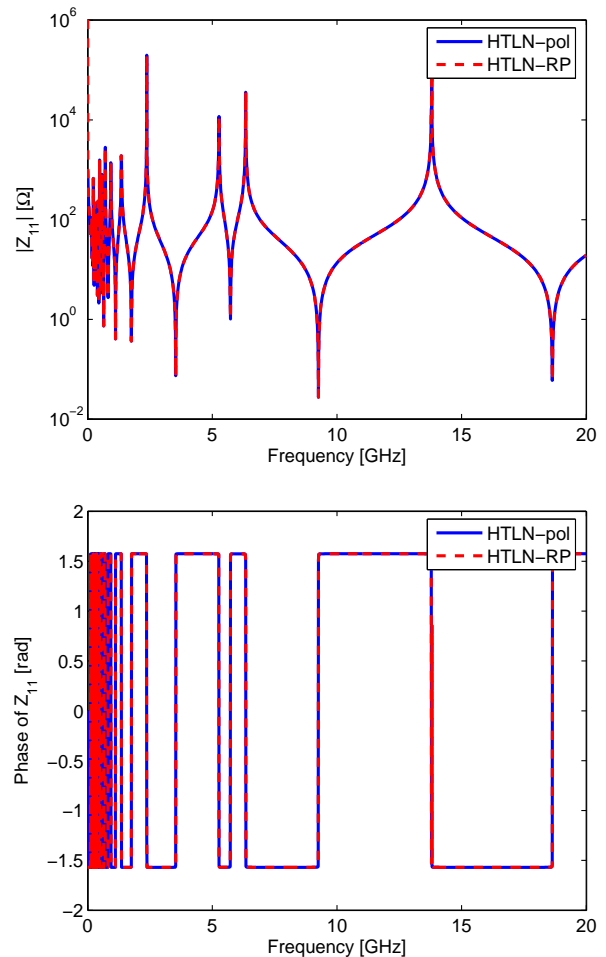

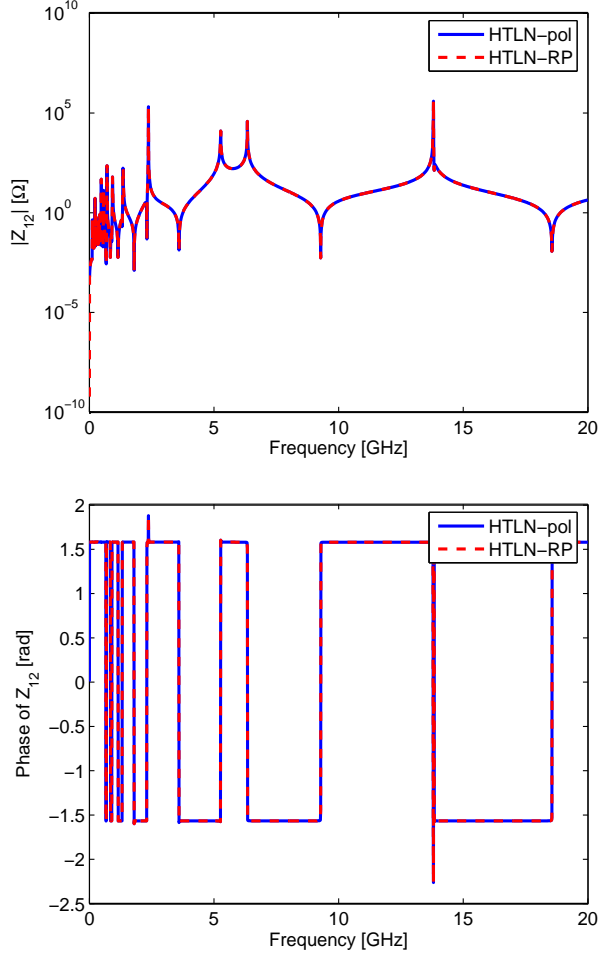Fig. 12.   Magnitude and phase spectra of Z_{11} (example V-B).

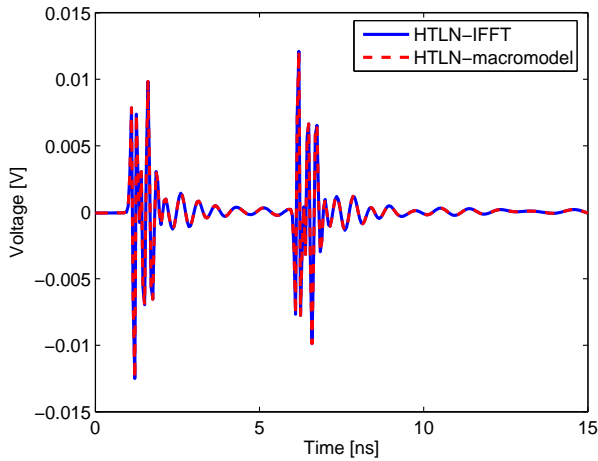Fig. 13. Magnitude and phase spectra of Z_{12} (example V-B).

Fig. 14. Port voltage V_2 (example V-B).

C. Four coupled CRLH-LNs

In the third test the CRLH-LN is obtained using four equally spaced coplanar microstrips ($\ell = 0.1\text{m}, \sigma =$

$5.8 \cdot 10^7$ S/m) on a alumina substrate ($\varepsilon_r = 9.8$). The cross section of the CRLH-LN structure is sketched in Fig. 15. The width of the strips is $w = 241$ μm, the spacing is $s = 800$ μm, the thickness of the dielectric and conductors are $h = 254$ and $t = 34.8$ μm, respectively, the shoulder $d = 2021.6$ μm. The computation of the per-unit-length parameters has been performed using the method of moments [23], yielding,

$$L_r = \begin{bmatrix} 0.3982 & 0.01369 & 0.00387 & 0.00203 \\ 0.01369 & 0.3979 & 0.01357 & 0.00387 \\ 0.00387 & 0.01357 & 0 - 3979 & 0.01369 \\ 0.002037 & 0.00387 & 0.01369 & 0.3982 \end{bmatrix} \mu\text{H/m} \tag{36a}$$

$$C_r = \begin{bmatrix} 172 & -0.5501 & -0.1206 & -0.0616 \\ -0.5501 & 172 & -0.5462 & -0.1206 \\ -0.1206 & -0.5462 & 172 & -0.5501 \\ -0.0616 & -0.1206 & -0.5501 & 172 \end{bmatrix} \text{pF/m}, \tag{36b}$$

$$R = \begin{bmatrix} 80.83 & 2.399 & 0.7926 & 0.4507 \\ 2.399 & 80.80 & 2.381 & 0.7926 \\ 0.7926 & 2.381 & 80.80 & 2.399 \\ 0.4507 & 0.7926 & 2.399 & 80.83 \end{bmatrix} \Omega/\text{m}, \tag{36c}$$

$$G = \begin{bmatrix} 0 & 0 & 0 & 0 \\ 0 & 0 & 0 & 0 \\ 0 & 0 & 0 & 0 \\ 0 & 0 & 0 & 0 \end{bmatrix} \text{S/m}. \tag{36d}$$
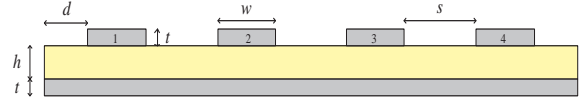

Fig. 15. Coplanar microstrips cross section (example V-C).

The microstrips are loaded with 15 longitudinal capacitances $C_L = 0.15$ nF and transverse inductances $L_L = 0.2$ μH.

The presence of the longitudinal capacitance C_L and the transverse inductance L_L causes a complex resonant behavior even at low frequency. Figure 16 shows an example of the magnitude spectrum of the input impedance Z_{11} evaluated using both the polynomial approach and the residue-pole form. The spectrum exhibits several resonances from 0 to 500 MHz while the inductive nature dominates at higher frequencies.

This fact is confirmed by the location of the poles in the complex plane, shown in Fig. 17. It is easy to recognize four families of poles, corresponding to four decoupled CRLH-LN and a cluster of poles close to zero determining the highly oscillating behavior at low frequency.
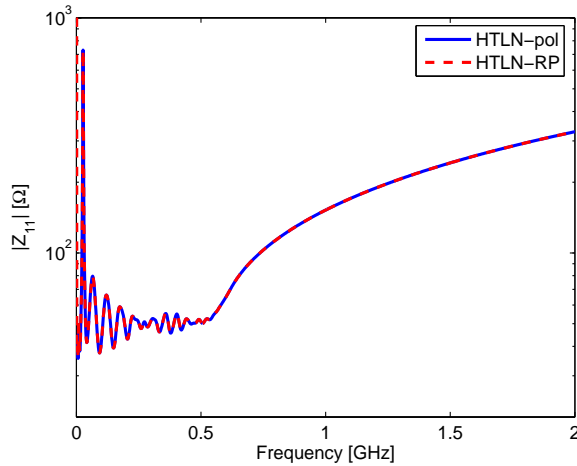
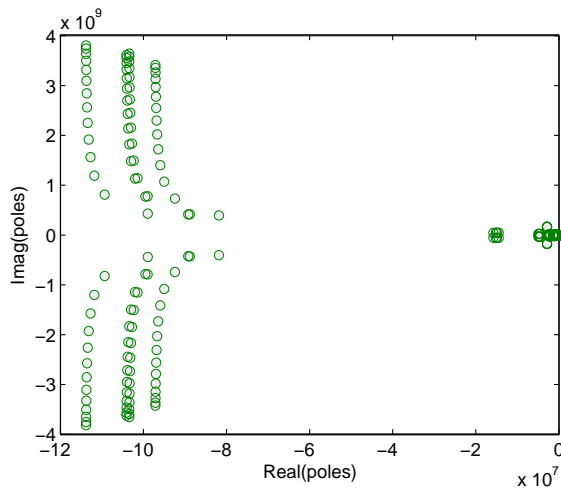Fig. 16.   Magnitude spectrum of impedance Z_{11} (example V-C).

Fig. 17.   Location of poles in the complex plane (example V-C).

Fig. 18.   Transient voltages at the output port of the first (top) and forth (bottom) CRLH-LNs (example V-C).

The rational macromodel has been generated in the state-space form. The four CRLH-LNs are terminated on 50 Ω at the input ports and 2 pF capacitances at the output ports. Figure 18 shows the transient voltages at the output of the first and fourth CRLH-LN as evaluated using the frequency-domain approach via inverse fast Fourier transform (HTLN-IFFT) and the proposed macromodel (HTLN-macromodel). Again, a very good agreement is obtained.

VI. CONCLUSIONS

In this work a systematic approach to coupled CRLH-LNs is presented. The closed-form two-port representation of CRLH-LNs is obtained relying on analytical polynomials whic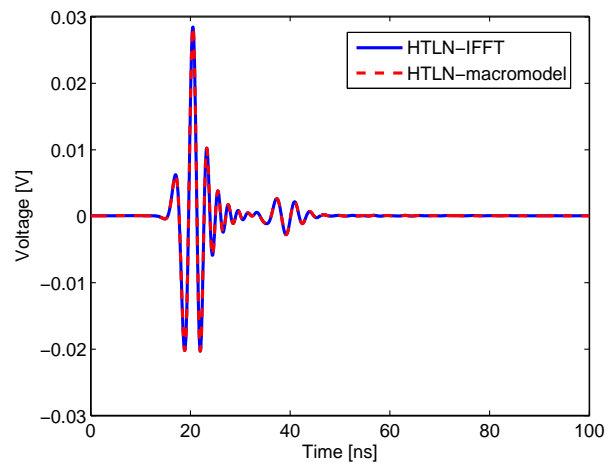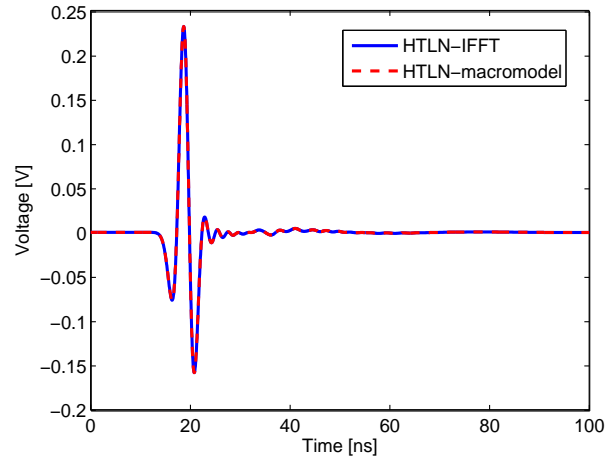h allow to exactly represent voltages and currents along the network. The rational form of the impedance matrix $\boldsymbol{Z}$ allows an easy identification of the true poles and the corresponding residues of the CRLH-LN and, thus, the generation of a rigorous state-space macromodel which is proved to be accurate from dc to daylight. Hence, the proposed method is well suited to represent N-coupled CRLH-LNs with general topology of longitudinal impedance $\boldsymbol{Z}_1$ and transverse admittance $\boldsymbol{Y}_2$. The presented numerical results have validated the method and confirmed its accuracy when compared with standard frequency-domain techniques.

REFERENCES

[1] V. G. Veselago, "The electrodynamics of substances with simultaneously negative values of ε and μ," *Sov. Phys. Usp.*, vol. 47, pp. 509–514, Jan.-Feb., 1968.

[2] C. Caloz and T. Itoh, "Transmission line approach of left-handed (LH) materials and microstrip implementation of an artificial LH transmission line,"

IEEE Transactions on Antennas and Propagation, vol. 52, no. 5, pp. 1159–1166, May 2004.

[3] ——, *Electromagnetic Metamaterials: Transmission Line Theory and Microwave Applications*. Wiley-IEEE Press, 2005.

[4] A. Lai, C. Caloz, and T. Itoh, "Composite right/left-handed transmission line metamaterals," *IEEE Microwave Magazine*, pp. 34–50, Sep. 2004.

[5] Y. Zhang and B. E. Spielman, "A stability analysis for time-domain method of moments analysis of 1-D double-negative transmission lines," *IEEE Transactions on Microwave Theory and Techniques*, vol. 55, no. 9, pp. 1887–1898, Sep. 2007.

[6] C. R. Paul, *Analysis of Multiconductor Transmission Lines*. New York, NY: John Wiley & Sons, 1992.

[7] A. Alù and N. Engheta, "Pairing an epsilon-negative slab with a mu-megative slab: resonance, tunneling and tranparency," *IEEE Transactions on Antennas and Propagation*, vol. 51, no. 10, pp. 2558–2570, Oct. 2003.

[8] ——, "Physical insight into the growing evanuescent fiels of double-negative metamaterial lenses using their circuit equivalence," *IEEE Transactions on Antennas and Propagation*, vol. 54, no. 1, pp. 268–272, Jan. 2006.

[9] G. V. Eleftheriades and K. G. Balmain, *Negative Refraction Metamaterials: Fundamental Principles and Applications*. Wiley-IEEE Press, 2005.

[10] P. P. So and W. J. R. Hoefer, "Time domain TLM modeling of metamaterials with negative refractive index," pp. 1779–1782, Jun 2004.

[11] A. Rennings, S. Otto, C. Caloz, A. Lauer, W. Bilgic, and P. Waldow, "Composite right/left-handed extended equivalent circuit," *Int. J. Numer. Model.*, vol. 19, pp. 141–172, 2006.

[12] R. F. Harrington, *Field Computation by Moment Methods*. Malabar: Krieger, 1982.

[13] G. Antonini, "Reduced order modeling for metamaterial transmission lines," *Applied Computational Electromagnetic Society Newsletter*, vol. 21, no. 3, pp. 78–103, Nov. 2006.

[14] H. V. Nguyen and C. Caloz, "Generalized couple-mode approach of metamaterial coupled-line couplers: coupling theory, phenomenological explanation and experimental demonstration," *IEEE Transactions on Microwave Theory and Techniques*, vol. 55, no. 5, pp. 1029–1039, May 2007.

[15] B. Gustavsen and A. Semlyen, "Rational approximation of frequency domain responses by vector fitting," *IEEE Transactions on Power Apparatus and Systems*, vol. 14, no. 3, pp. 1052–1061, Jul. 1999.

[16] D. Deschrijver, B. Haegeman, and T. Dhaene, "Orthonormal vector fitting : a robust macromodeling tool for rational approximation of frequency domain responses," Feb. 2007.

[17] D. Deschrijver, T. Dhaene, "Broadband macromodelling of passive components using orthonormal vector fitting," *Electronics Lett.*, vol. 41, no. 21, pp. 1160–1161, Oct. 2005.

[18] G. V. Eleftheriades, O. Siddiqui, and A. K. Iyer, "Transmission line models for negative refractive index media and associated implementations without excess resonators," *IEEE Microwave and Wireless Components Letters*, vol. 13, no. 2, pp. 51–53, Feb. 2003.

[19] J. Vlach and K. Singhal, *Computer Methods for Circuit Simulation*. Van Nostrand Reinhold Co, New York, 1983.

[20] M. Faccio, G. Ferri, and A. D'Amico, "A new fast method for ladder networks characterization," *IEEE Transactions on Circuits and Systems, I*, vol. 38, no. 11, pp. 1377–1382, Nov. 1991.

[21] M. Faccio, G. Ferri, A. D'Amico, "The DFF and DFFz triangles and their mathematical properties," *Applications of Fibonacci Numbers, G. E. Bergum et al.,(eds)*, vol. 5, pp. 199–206, 1990.

[22] E. W Weisstein, "Quartic Equation," *Mathworld–A Wolfram Web Resource*, http://mathworld.wolfram.com/QuarticEquation .html.

[23] A. R. Djordjevic, M. B. Bazdar, T. K. Sarkar, and R. F. Harrington, *Matrix parameters for multiconductor transmission lines*. Boston London: Artech House Publishers, 2000.

Giulio Antonini received his Laurea degree (summa cum laude) in Electrical Engineering in 1994 from the Università degli Studi dell'Aquila and the Ph.D. degree in Electrical Engineering in 1998 from University of Rome "La Sapienza". Since 1998 he has been with the *UAq EMC Laboratory*, Department of Electrical Engineering of the University of L'Aquila where he is currently Associate Professor. His research interests focus on EMC analysis, numerical modeling and in the field of signal integrity for high-speed digital systems. He has authored or co-authored more than 120 technical papers and 3 book chapters. Furthermore, he has given keynote lectures and chaired several special sessions at international conferences. He has been the recipient of the IEEE Transactions on Electromagnetic Compatibility Best Paper Award in 1997, the CST University Publication Award in 2004, the IBM Shared University Research Award in 2004, 2005 and 2006; in 2006 he has received a Technical Achievement Award from the IEEE EMC Society "for innovative contributions to computational electromagnetic on the Partial Element Equivalent Circuit (PEEC) technique for EMC applications". He holds one European Patent.Prof. Antonini is vice-chairman of the dell'IEEE EMC Italy Chapter, he is member of the TC-9 committee and vice-chairman of the TC-10 Committee of the IEEE EMC Society. Prof. Antonini serves as reviewer in a number of international journals.